

Eclipse timing Variations Of Planets In P-Type Binary Star Systems

R. Schwarz¹, N. Haghighipour², S. Eggl¹, B. Funk³, and E. Pilat-Lohinger¹

¹) Institute for Astronomy, University of Vienna, A-1180 Vienna, Türkenschanzstrasse 17, Austria; ²) Institute for Astronomy and NASA Astrobiology Institute, University of Hawaii-Manoa, Hawaii, USA ; ³) Department of Astronomy, Eötvös University, H-1117 Budapest, Pázmány Péter setany 1/A, Hungary

ACKNOWLEDGMENTS

Supports through the MOEL grant of the ÖFG (Project MOEL 386) and the FWF project P18930 for R.S., the NASA Astrobiology Institute for N.H., the Austrian FWF Erwin Schrödinger grant no. J2892-N16 for B.F., the Austrian FWF project no. P20216 for S.E. and the Austrian FWF projects no. P20216 and P22603 for E. P-L.

REFERENCES

Rabl, G. & Dvorak, R., 1988, A&A, 191, 384; Schneider, J. & Chevreton, M., 1990, A & A, 232, 251.; Sybilski, P., Konacki, M. and Kozłowski, S., 2010, MNRAS, 405, 657.

1 INTRODUCTION

Approximately 70 percent of all stars in the solar neighborhood are members of binary or multiple star systems. This fact has led to speculations that many more planets may exist in binary stars, and that the knowledge of the dynamics of planets in binary systems is crucial. In general, one can distinguish different types of stable orbits for planets in binary systems (Rabl & Dvorak 1988) (Figure 1):

- (i) S-Type, where the planet orbits one of the two stars,
 - (ii) P-Type, where the planet orbits the entire binary.
- We focus on P-Type orbits, because many of close eclipsing binaries lie in the CoRoT discovery space.

Eclipse timing variations (ETVs):

We calculated ETVs for the transiting star by subtracting the time of the eclipse of the unperturbed case (t_1 , star-star configuration) from the perturbed case (t_2 star-star-planet configuration). Subtraction of the constant rate of apsidal precession yields the eclipse timing variation δt .

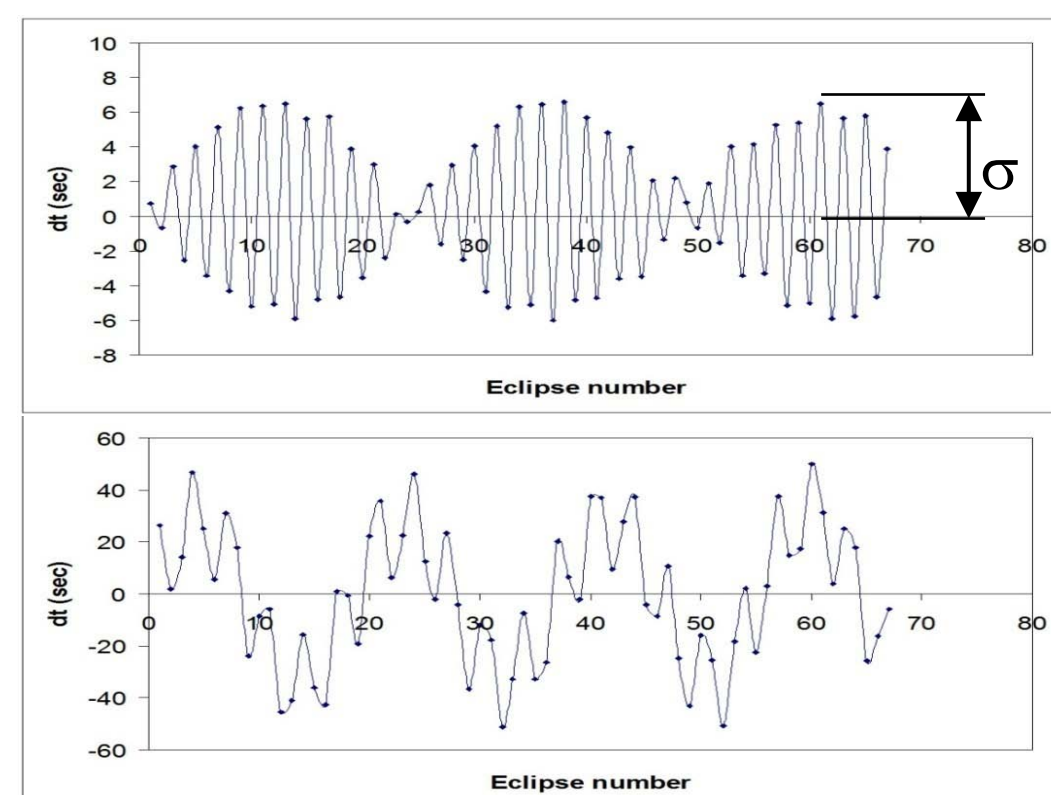


Figure 4. ETVs for circular orbits of the planet using model 3 for the 3:1 resonance (upper graph) and the 4:1 resonance caused by a planet of $1 M_J$. The x-axis shows the number of transits whereas the y-axis depicts the timing variation (δt).

4 RESULTS

Our goal was to show which kind of planets are detectable via observation of the ETV signal with current observational equipment. We compared the expected **amplitude of the ETV** signal $\sigma = (dt_{\max} - dt_{\min})/2$ to the detection limit of current space observatories. The maximum σ for CoRoT (at $L=15.5$ mag) and Kepler (at $L=14.5$ mag), are shown in Figure 5 as full line (Kepler) and dashed line (CoRoT) (Sybilski et al. 2010). If the ETV signal is higher than the observational threshold, we can assume that a planet will be indirectly detectable by Eclipse timing measurements of the secondary star.

We could show, that **planets around sun-like binary systems also produce ETV signals significant enough to be detected**. In that case the planets have to be on a circular orbit very close to the secondary star $a = 2 a_{\text{bin}}$ or – in case of planets with $a > 2 a_{\text{bin}}$ they have to be more massive ($m > 5 M_J$). Finally calculations were performed to check whether it is possible to detect **Earth-like** or Super-Earth planets. We used the closest possible distance ($a = 2 a_{\text{bin}}$), with initial conditions given in Table 1. The investigations show the following results: For **model 1** with $1 M_E$ we have $\sigma = 3$ sec, $5 M_E$ results in $\sigma = 6$ sec and with $10 M_E$ we get $\sigma = 22$ sec. In addition **model 2** showed a detectable ETV signal for Kepler with $10 M_E$ ($\sigma = 8$ sec). Further investigations have to be done including the respective orbital inclination between the binary and its planet.

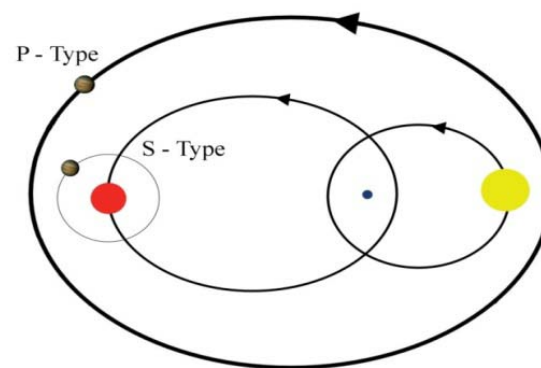


Figure 1. Schematic of S and P-type binary configurations

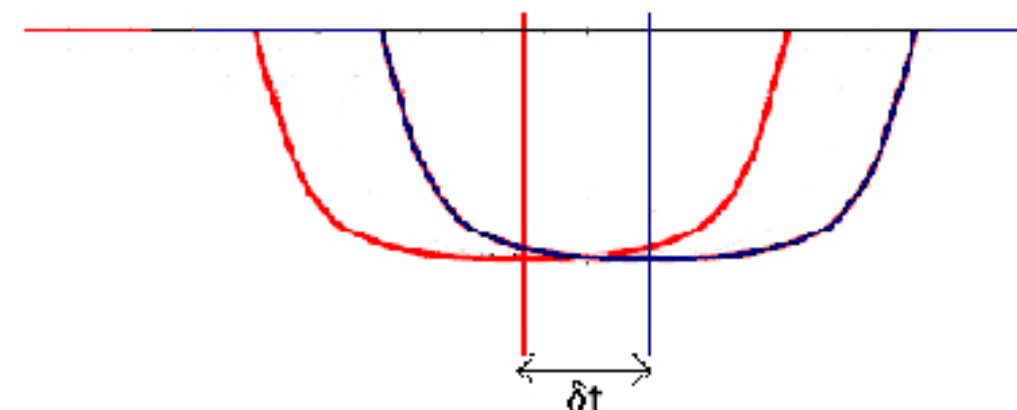


Figure 2. A non constant variability in the exact moment of a binaries' eclipse caused by e.g. a perturbing planet is known as eclipse time variation (δt)

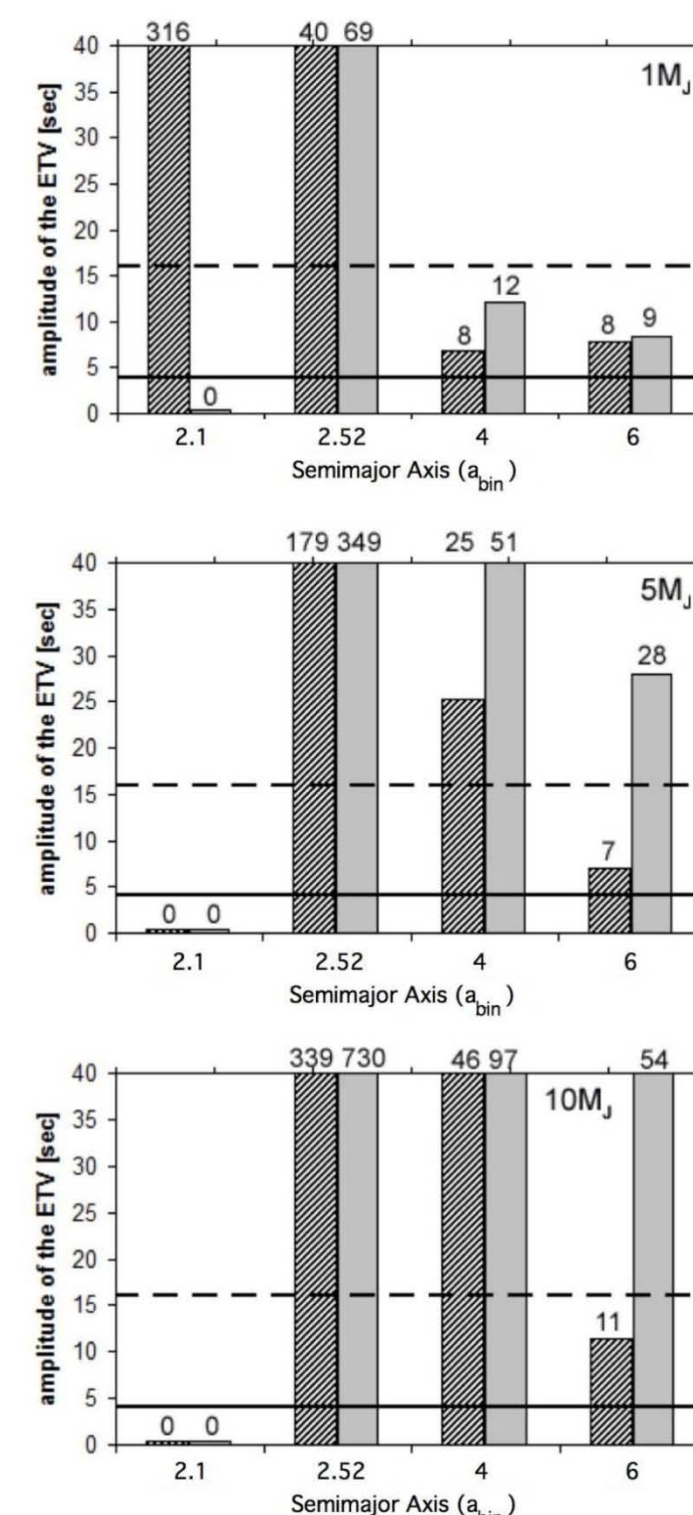


Figure 5. Results for all ETVs for **model 1**. The upper graph present calculations for $1 M_J$ the middle one for $5 M_J$ and the lower one for $10 M_J$. The x-axis depicts the initial semi-major axis of the planet whereas the y-axis depicts **amplitude of the ETV**.



2 MODELS AND METHODS

Our numerical simulations were carried out using the following two integration methods (a) the Lie-Series and (b) the Bulirsch-Stoer method. For the analysis of the stability we used the Fast Lyapunov Indicator (FLI) on the one hand and on the other hand the maximum eccentricity (e_{\max}). For the e_{\max} we examined the behaviour of the eccentricity of the planet along the integration. If the orbit becomes parabolic (i.e. $e_{\max}=1$), the system is considered to be unstable. All numerical simulations used the full three-body problem as a dynamical model; here m_1 is the primary star, m_2 the secondary star and m_3 the planet. We used 3 different types of binaries (sorted by total mass):

- model 1:** $m_1 = m_2 = 0.3 M_{\text{sun}}$
- model 2:** $m_1 = 1, m_2 = 0.5 M_{\text{sun}}$
- model 3:** $m_1 = m_2 = 1 M_{\text{sun}}$

The initial conditions for the planet are given in Table 1. Additionally we included some test calculations for ETVs of Earth and Super-Earth like bodies.

	a_p/a_{binary}	e	$M_{\text{planet}} [M_J] \cdot [M_E]$	i, ω, M, Ω [deg]
stability map	2–6	0.1–0.3	1, 5, 10	0
grid-size	$\Delta a = 0.01$ [AU]	$\Delta e = 0.01$		
ETV	2.1, 2.52, 4, 6	0, 0.3	1, 5, 10	0
ETV	2.1	0	*1, *5, *10	0

Table 1. Grid of initial conditions for the planet m_3 . $M_J = 1$ Jupiter mass, $M_E = 1$ Earth mass.

3 STABILITY OF THE SYSTEMS

The stability study for the different models was necessary in order to identify stable configurations for the analysis of the ETV signals. We used a separation of the binary of $a=0.05$ AU which corresponds to a period of approximately 3 days for sun mass stars ($1 M_{\text{sun}}$) and 5 days for stars with $0.3 M_{\text{sun}}$.

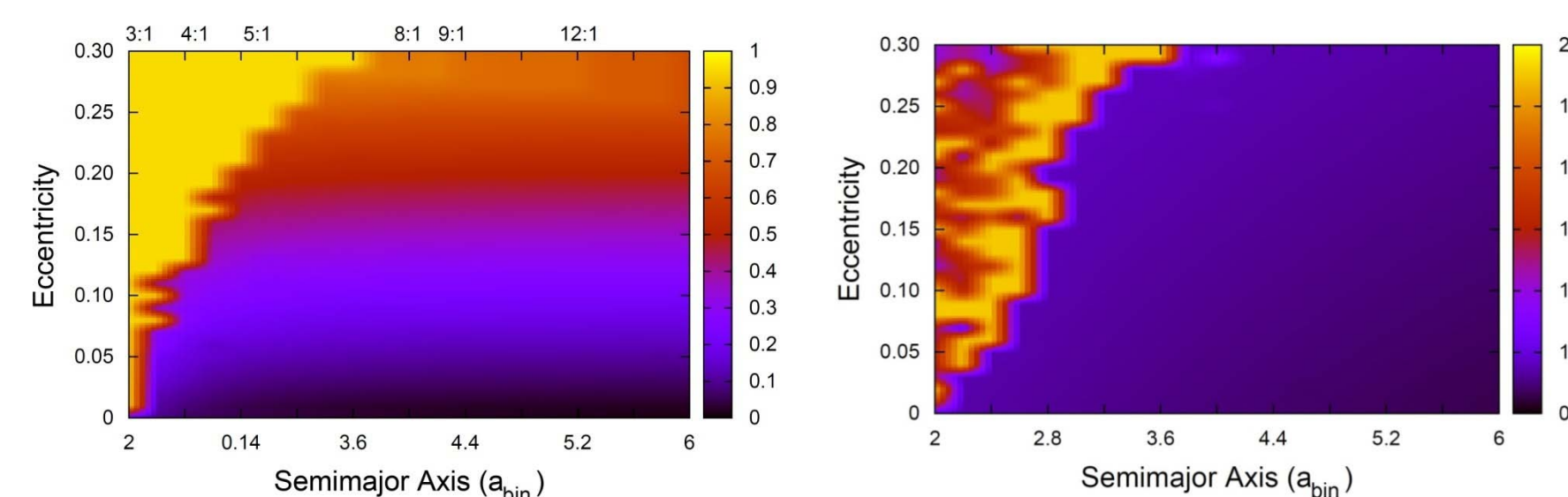


Figure 2. Stability map for $1 M_J$ for **model 1**. The stability was investigated by the e_{\max} (left) and the FLI (right). The violet and blue region depicts stable and the yellow region chaotic motion.

The stability analysis showed, that there is a large region for planets in stable P-type motion around binary stars. The stability maps do not point to any mean motion resonance (MMR), but the ETVs do, namely in the cases of the 3:1 MMR and the 4:1 MMR. We found, that the stable region shrinks rapidly with higher eccentricities of the secondary star. For initial conditions beyond $e_{\text{bin}} = 0.15$ we could not find stable orbits and therefore we did not investigate ETV signals in such systems. Our results have shown, that binary systems with low mass stars are good candidates to discover new planets via Eclipse timing of the secondary.

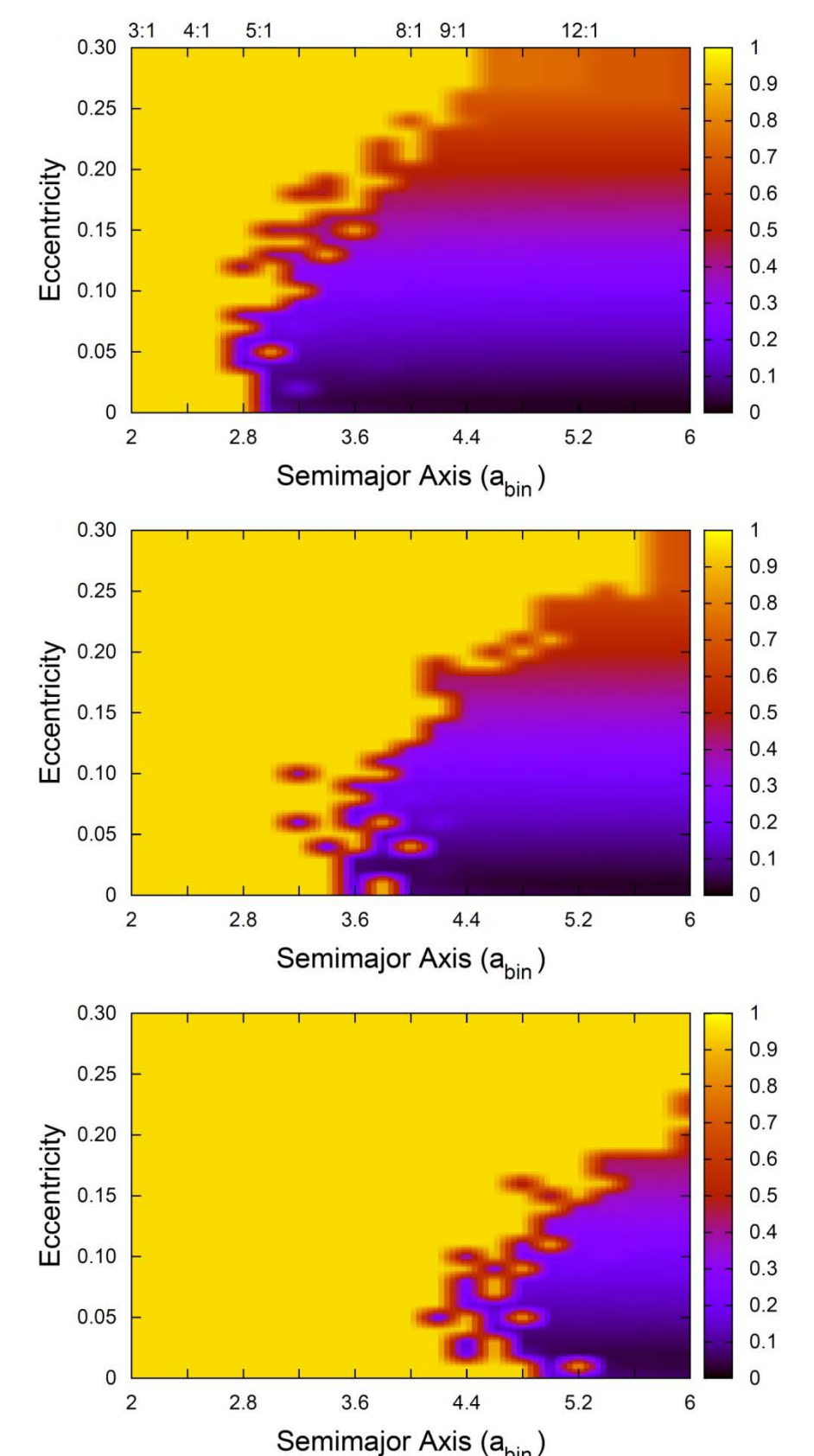


Figure 3. Stability map for $e_{\text{bin}} = 0.05$ (upper graph), $e_{\text{bin}} = 0.10$ (middle graph) and $e_{\text{bin}} = 0.15$ (lower graph) for **model 1** with a planet of $1 M_J$. The stability is given by the e_{\max} , where the violet and blue region (small values e_{\max}) depicts stable motion and the yellow region chaotic motion.